JACS
JOURNAL OF THE AMERICAN CHEMICAL SOCIETY

ARTICLE

pubs.acs.org/JACS

Effect of Urea on the β-Hairpin Conformational Ensemble and Protein Denaturation Mechanism

Anna Berteotti, Alessandro Barducci,* and Michele Parrinello

Computational Sciences, Department of Chemistry and Applied Biosciences, ETH Zurich, USI Campus, Via Giuseppe Buffi 13, CH-6900 Lugano, Switzerland

Supporting Information

ABSTRACT: Despite the daily use of urea to influence protein folding and stability, the molecular mechanism with which urea acts is still not well understood. Here the use of combined parallel tempering and metadynamics simulation allows us to study the free-energy landscape associated with the folding/unfolding of β-hairpin GB1 equilibrium in 8 M urea and pure water. The nature of the unfolded state in both solutions has been analyzed: in urea solution the addition of denaturants acts to expand the denatured state, while in pure water solution the unfolded state is noticeably more compact. For what concerns the mechanism by which urea acts as a denaturant, a preferential direct interaction between urea molecules and protein backbone has been found. However, the bias toward urea solvation is largest at intermediate values of the gyration radius.

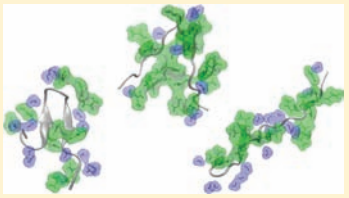

INTRODUCTION

A protein folds as a result of a delicate balance of forces between the interactions within the protein and with its environment. Protein molecules in aqueous buffer are in equilibrium between unfolded (U) and native (N) states, U ⇌ N.[1,2] This balance can be perturbed in different ways, by temperature, pressure, pH, or the presence of organic molecules. Urea is a small hydrophilic molecule, present in all taxa. It is a widely used protein denaturant in *in vitro* experiments. However, despite its everyday use in the study of protein folding and stability, the molecular mechanism by which urea acts is still not well understood. In particular, the question of which kind of interactions are the main driving forces for urea-induced denaturation has been intensively studied. Two main mechanisms of action have been proposed: (1) an "indirect mechanism" in which urea disrupts the structure of water, thus promoting the solvation of hydrophobic groups[3−5] or (2) a "direct mechanism" in which urea interacts directly with the protein.[6−19] In the direct mechanism urea can interact either directly with the protein backbone, via hydrogen bonds (H-bonds) and other electrostatic interactions, or with the amino acids by more favorable van der Waals attractions, or with both, thus causing the protein to open and denature.

Within the supporters of the direct mechanism, opinions are further divided between those who underline the role of electrostatic interactions[8−14] and those who favor the role of the hydrophobic interaction.[15−19] Thus, contrasting conclusions have been reached using a combination of experimental data and atomistic molecular dynamics (MD) simulations. However, due to the limited simulation time, only partial unfolding events could be observed in these earlier simulations and often high temperature were used to accelerate unfolding.

More recently the time scale has been increased to a few microseconds, and in lysozyme a two-step process has been found.[20] While highly illuminating, these calculations did not report any free-energy calculations. Efforts at improving sampling have also been recently made by Canchi et al.,[21,22] who have used replica exchange to study the folding equilibrium of the Trp cage protein in the presence of urea, finding, in agreement with experiments, a linear dependence of the unfolding free-energy on urea concentrations. The authors have described the nature of the folded and unfolded states at different urea concentrations; however, the structural transition between the two ensembles was not described, and possible intermediate states were not characterized.

To shed more light on the effect of urea, we report the folding/unfolding equilibrium of the 16-residue C-terminal fragment of protein GB1 (β-hairpin) in 8 M urea and pure water obtained by means of the combination of metadynamics[23] and parallel tempering (PTMetaD).[24] The use of these two combined methods allows an improvement of the capability of both: metadynamics improves the ability of parallel tempering to explore low-probability regions, leading to a more reliable description of the free-energy landscapes. On the other hand, parallel tempering allows sampling the degrees of freedom not explicitly included in the collective variables (CVs), thus improving the metadynamics accuracy. To understand in depth the nature of urea−protein interactions, we used a newly developed reweighting algorithm that allows to recover from a well-tempered metadynamics[25] simulation the equilibrium probability distribution of any variable.[26]

Here, for the first time, we can not only describe the folding mechanism but also determine the free-energy landscape. As expected, we find that in urea solution the U ⇌ N equilibrium is shifted toward the unfolded state with respect to the water system.

Received: March 29, 2011
Published: August 19, 2011

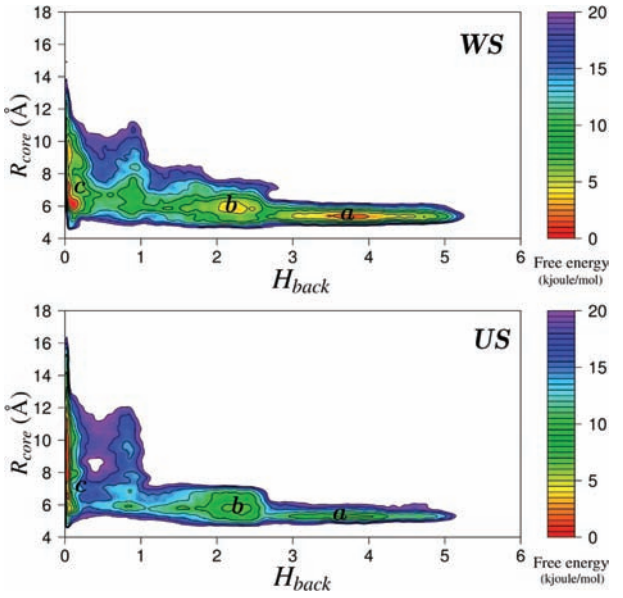

Figure 1. FES as a function of H_{back} of the parallel β-sheet and R_{core} calculated on the hydrophobic core of the protein. The upper panel corresponds to WS, while the lower panel corresponds to US. Contour lines are plotted every 5 kJ/mol, and the color legend is in kilojoules per mole.

The nature of the unfolded state is different in the two solutions: in urea the unfolded structure is much more elongated than in water. In agreement with ref 20, we find that also the GB1 β-hairpin has a two-step unfolding mechanism. First, urea directly interacts with the protein backbone through H-bonds, retaining a compact form with a low gyration radius. Then the protein unfolds in a stretched conformation with high values of the gyration radius.

RESULTS AND DISCUSSION

Free-Energy Landscape. In Figure 1 the free-energy landscapes (FESs) as a function of two CVs, the radius of gyration calculated on the hydrophobic core (R_{core}), and the number of intramolecular backbone−backbone H-bonds (H_{back}) at room temperature, obtained by means of PTMetaD for the two solutions under investigation, are reported.

The FES was reconstructed from 100 ns of PTMetaD simulation in the case of 8 M urea solution (US) and from 70 ns of simulation in the case of water solution (WS).

The FESs in both cases exhibit quite similar L-shapes. This indicates similar zipping mechanisms in which native contacts must first be broken before the protein loses its hydrophobic core and goes into a stretched conformation. Going from the folded (a) to the unfolded (c) state, the protein breaks the H-bonds of the backbone before losing the hydrophobic core. A comparison of these FESs and that reported by Bussi et al.[24] shows that the overall mechanism is quite similar; in fact also in ref 24 there is an L-shaped FES. However, in our case, in both solutions, there is a minimum (b) that was not present in ref 24. We attribute this to the different force field used, Amber99SB[27] against OPLS-AA[28] in ref 24.

This minimum corresponds to structures intermediate between the native and the unfolded states: the protein still has some elements of secondary structure; particularly, the first β-sheet H-bonds closest to the turn region are still formed. At values of H_{back} smaller than 1, we can see in both cases the presence of a broad minimum that represents the unfolded state.

The differences between the two solutions are to be seen in the depths of the minima. In fact, while the localization of the minima are almost similar in both cases, their depths are different. As expected, WS stabilizes the folded state, while US stabilizes the unfolded state. From these FESs it is not trivial to understand the differences between the two environmental conditions on the folding−unfolding equilibrium of the β-hairpin protein. In fact the CVs, while extremely useful at accelerating sampling, have a low resolution at small H_{back}, which is the region of the unfolded state. For these reasons we reconstructed the FES by means of the newly developed reweighting mechanism as a function of different collective variables which are able to explore this region in greater detail.

Using ref 26, we plot the FESs as a function of the radius of gyration calculated on the Cα atoms of the protein (R_{ca}) and the distance from the crystallographic state in contact map space (Z_{map}) (see the Methods for details). The resulting FESs are shown in Figures 2 and 3.

It is to be seen in Figures 2 and 3 that basins a and b of Figure 1 in both solutions are preserved and are now mapped into minima 1 and 2. As wished for, basin c is now resolved in different local minima, especially in US (Figure 3). As expected, in US the equilibrium between folded and unfolded states is shifted toward the disordered state. According to these FESs, the folding free-energy ΔF_{FU} is in WS ∼0 kcal/mol and in US ∼1 kcal/mol. The convergency plot of ΔF_{FU} can be found in the Supporting Information. These results are in remarkable agreement with NMR experiments which suggest that the population of the β-hairpin structure is 42% in water[29,30] and 23% in 6 M urea.[31] The ensemble of the unfolded state is different in the two cases, and it is seen that the gyration radius is larger in US and several likely structures can be found with a radius of gyration that ranges from 8 to 12 Å. Several experiments have shown that the unfolded state in urea solution is considerably more extended than when denaturation is induced by other agents such as pH or temperature.[32−35] Moreover, recent single-molecule FRET experiments showed an increase of the radius of gyration of the unfolded state for different proteins with increasing denaturant concentration.[36,37] This qualitative agreement between theory and experiment reassures us on the validity of our model. Thus, with some confidence we can proceed further in the analysis to get a deeper insight into the role of urea.

Role of the Solvent in WS and US. An important insight into the nature of the unfolding mechanism comes from the study of the interaction between the solvent and the protein. First, we examine the interactions between the protein backbone and solvent in terms of the number of H-bonds, and then we study the effect of the solvent on the packing of the hydrophobic side chain. In Figure 4A,B we report the FESs as a function of the distance from the crystallographic structure in contact map space (Z_{map}) and Cα gyration radius (R_{ca}) colored according to the average number of H-bonds between the backbone and the solvent ($HB_{bb-solv}$). We consider all the possible H-bonds between the backbone polar groups and all the solvent molecules in both solutions. From panels A and B it is clear that there is a different pattern of solvation in US compared to WS and that the backbone polar groups in the unfolded state are more solvated in US. A similar behavior was not observed (see the Supporting Information) for the interaction between the solvent and the side chains polar groups.

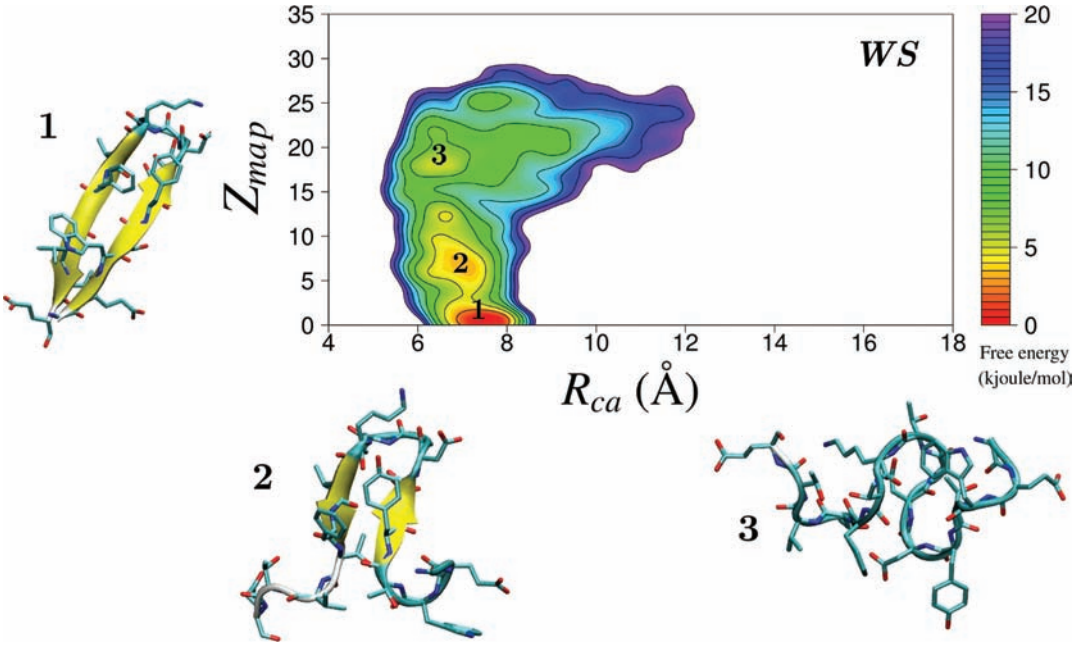

Figure 2. Reconstructed FES for WS as a function of the distance from the crystallographic state in contact map space (Z_{map}) and R_{ca} calculated on Cα atoms of the protein. Contour lines are plotted every 2 kJ/mol, and the color legend is in kilojoules per mole. Images 1−3 of WS show the typical structures encountered in such minima.

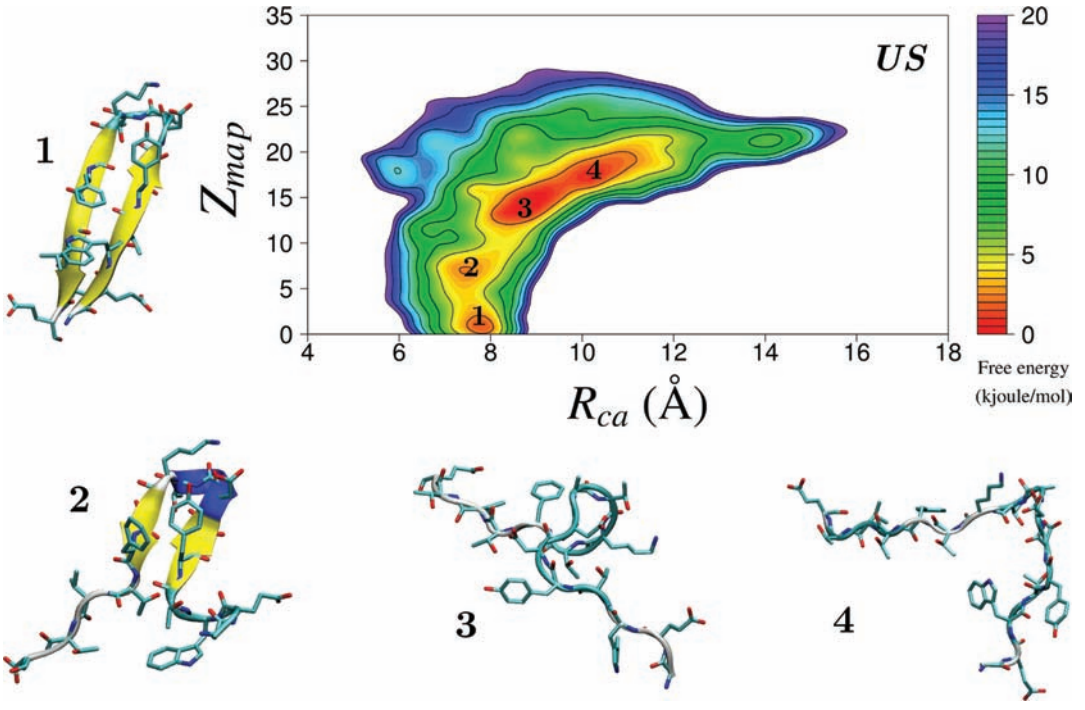

Figure 3. Reconstructed FES for US as a function of the distance from the crystallographic state in contact map space (Z_{map}) and R_{ca} calculated on Cα atoms of the protein. Contour lines are plotted every 2 kJ/mol, and the color legend is in kilojoules per mole. Images 1−4 of US show the typical structures encountered in such minima.

We further report the average $HB_{bb-solv}$ as a function of the gyration radius only (Figure 4D). In US even the compact states are more solvated, and this trend is further enhanced at intermediate values of R_{ca} where the protein is partially open. When the protein is totally stretched, this difference tends to be much reduced. It is also instructive to analyze the formation of total and non-native backbone−backbone H-bonds (Figure 4D). In particular, in WS the average number of intramolecular H-bonds decays more slowly than in US, and a larger number of non-native contacts are found in the intermediate R_{ca} regime. This indicates a greater resilience of the system to solvation in pure water and suggests the existence of different intermediate structures in the

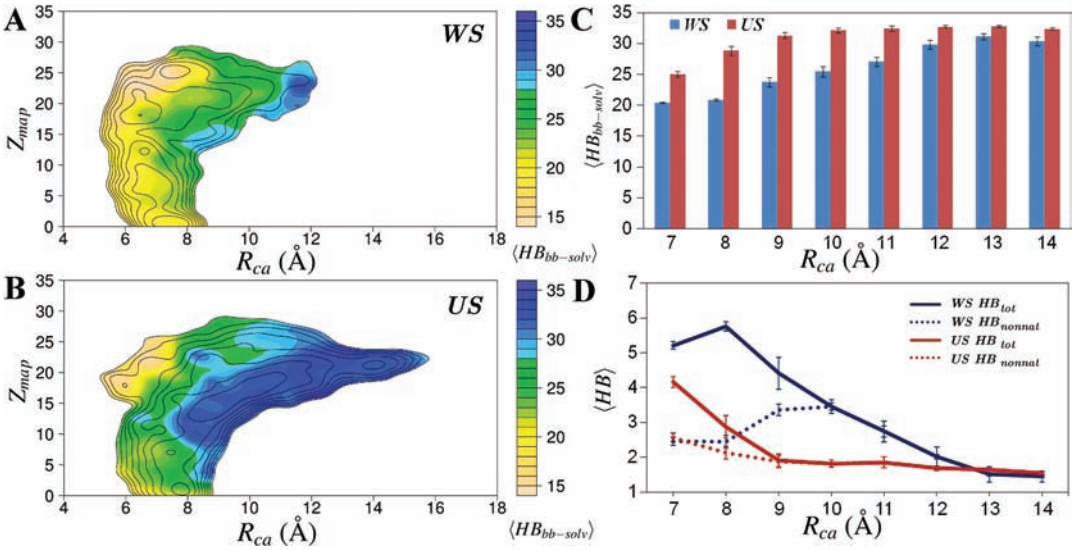

Figure 4. Role of the solvent. The FESs as a function of the distance from the crystallographic structure in contact map space (Z_{map}) and Cα gyration radius (R_{ca}) colored according to the average number of H-bonds between the backbone and the solvent ($HB_{bb-solv}$) are reported in panels A and B. The free-energy surfaces are plotted with contour lines, every 2 kJ/mol, and a color scale representing the average $HB_{bb-solv}$. (A) corresponds to WS, while (B) corresponds to US. The histogram in (C) represents the average $HB_{bb-solv}$ in the two solutions; blue corresponds to WS and red to US. In (D) is reported the averaged number of H-bonds within polar groups of the backbone: blue refers to WS and red to US. In solid lines the total number of intramolecular H-bonds (HB_{tot}) is reported, while in dashed lines the non-native intramolecular H-bonds (HB_{nonnat}) can be seen.

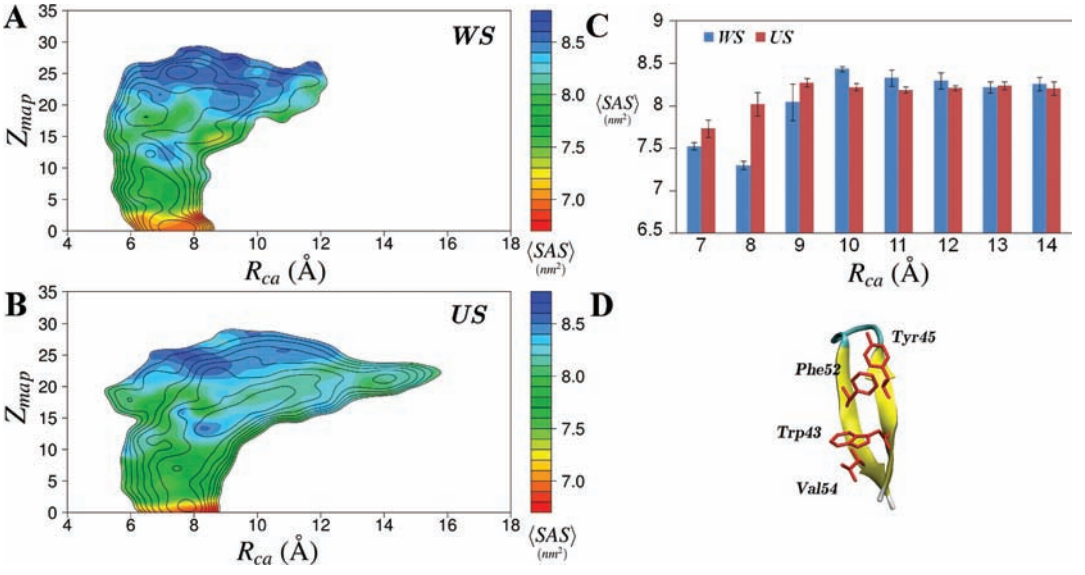

Figure 5. Hydrophobic effect. (A) and (B) depict the FES as a function of Z_{map} and R_{ca} colored according to the average *SAS*. The free-energy surfaces are plotted with contour lines, every 2 kJ/mol, and a color scale representing the averaged number of *SASs*. (C) shows the averaged number of *SASs* along the progress of R_{ca}. In (D) the native state of the β-hairpin protein is reported; in red the four amino acids that form the hydrophobic core are highlighted.

two solutions.[38] We also studied the effect of the solvent on the hydrophobic core in the two solutions.

In Figure 5 we report the FESs as a function of Z_{map} and R_{ca} colored according to the average solvent-accessible surfaces (*SASs*) of the hydrophobic core. The *SAS* of the hydrophobic core describes how the side chains of the hydrophobic residues are mutually coordinated in the space. Low values of *SAS* correspond to a highly packed hydrophobic core, while high values indicate the disruption of the core.

When the protein backbone is close to the crystallographic structure (low values of Z_{map}), the average conformations of the hydrophobic core are different in the two solutions. In particular, it can be seen that in WS the core is preferentially in a closed conformation whereas in US the presence of urea prevents the collapse of the core. In other regions of the conformational space the behaviors of the hydrophobic core in the two solutions are rather similar. This trend is confirmed by the average value of *SAS* as a function of R_{ca} (Figure 5C), which indicates that only for the

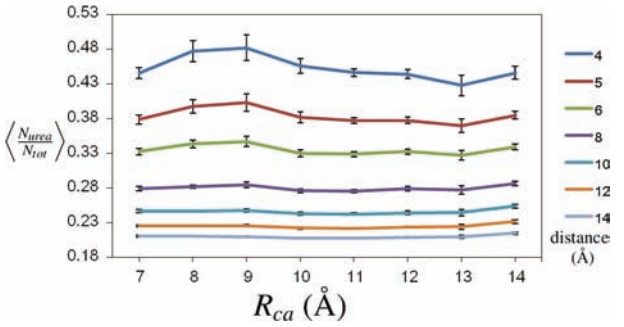

Figure 6. Urea concentration calculated at different distances from the Cα atoms as a function of R_{ca}. We included all the water and urea molecules with at least one atom within the reported distances.

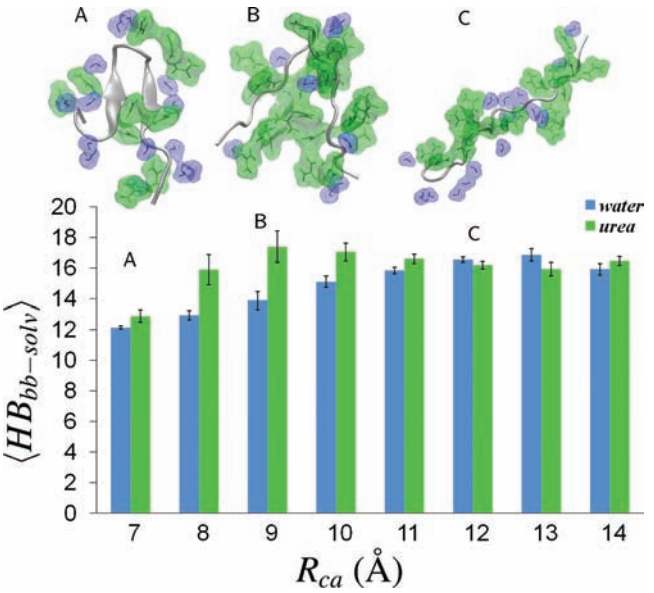

Figure 7. Averaged number of H-bonds formed between the backbone and urea are reported in green, in blue that between the backbone and water. Three typical structures encountered at values of 7, 9, and 12 of R_{ca} are reported in images A, B, and C.

most compact configurations the hydrophobic side chains are more exposed to the solvent in US than in WS.

As already mentioned in the Introduction, it is a matter of discussion if in the interaction between urea and protein the polar or the apolar components dominate. In particular, the relative importance of protein−solvent H-bonds and van der Waals interactions in the unfolding process has been discussed.[12,14−19]

Our data clearly indicate that the urea-driven denaturation of the GB1 β-hairpin mainly involves the formation of H-bonds between the solvent and the backbone polar groups while only a smaller role can be assigned to the weakening of hydrophobic interactions. It must be pointed out that, even if these results might be specific to the small system studied here, they are in good agreement with recent experimental and theoretical studies[39,40] on larger proteins.

Urea's Mechanism of Action in 8 M Urea Solution. To evaluate which is the main force that stabilizes the formation of the US unfolded state, we have studied the role of the two cosolvents. In Figure 6 the ratio between the numbers of urea and water molecules is reported as a function of R_{ca} and the distance from the protein Cα atoms.

Going closer to the protein, from 14 to 4 Å the local urea concentration increases, suggesting a preferential direct interaction of urea with the protein backbone as compared to water.

Moreover, it must be noted that the local urea concentration at short distance from the protein exhibits a maximum for conformations corresponding to R_{ca} around a value of 9 Å . This suggests the presence of a state with intermediate values of R_{ca} where the backbone−urea interaction is maximal. To get a deeper insight into this behavior, we report in Figure 7 the total number of hydrogen bonds between the protein backbone polar groups and solvent molecules per species. In analyzing these data one must keep in mind that, while urea can form a larger number of H-bonds, its concentration is much smaller. Thus, a comparable $HB_{bb-solv}$ indicates a stronger propensity of urea to bind to the protein backbone. As shown in Figure 7 along the whole range of R_{ca}, urea preferentially interacts with the protein backbone as compared to water.

Going from the folded to the unfolded state, the whole range of R_{ca} can be split into three main regions. The first one, A, corresponds to very compact conformations where also the folded state lies. The interactions between urea and water molecules are comparable. Going into the second region, say from a 8 Å to a 9 Å value of R_{ca}, there is an increased number of H-bonds between the backbone and urea compared to water, while in the third region, C, the water and urea backbone interactions are again similar. Representative snapshots of the environment behavior around the protein at values of 7, 9, and 12 Å of R_{ca} can be seen in the upper panel of Figure 7.

This behavior, along the unfolding pathway, means that when the protein starts to unfold and reaches a more elongated conformation, there is a scarcity of water molecules around it while urea can more easily interact. The presence of intermediate conformations during the first stages of the unfolding process with an increased interaction with urea has already been suggested by another study[20] based on a single long MD simulation of lysozyme in 8 M urea. These authors proposed a two-stage unfolding process with urea penetrating the hydrophobic core before water, forming a "dry globule" intermediate state. Here, equilibrium simulations of the folding/unfolding pathway of the β-hairpin confirm this observation by proving the existence of a state at intermediate value of R_{ca} in which urea interaction with the protein backbone and local concentration is maximal.

CONCLUSIONS

The use of advanced sampling techniques has allowed us a deeper understanding of the main differences in the reversible folding−unfolding free-energy landscape of β-hairpin GB1 in 8 M urea solution and pure water. The folding free-energy ΔF_{FU} for the two solutions has been calculated: as expected, the equilibrium between folded and unfolded states is shifted in US toward the disordered one in qualitative and quantitative agreement with NMR experiments. The nature of the unfolded states has been extensively analyzed: our data show that urea stabilizes the protein in a completely unfolded conformation, with high values of the gyration radius. This behavior confirms that the addition of denaturants allows the protein to unfold in a stretched conformation. In the absence of denaturant, the unfolded state is in equilibrium with the native state and it is noticeably more compact.

For what concerns the mechanism by which urea acts as a denaturant, the main role is played by the preferential direct interaction between urea molecules and the protein backbone through H-bonds. The number of these interactions is indeed maximized even after minimal protein expansion. Furthermore, considering the ratio of urea−backbone over water−backbone H-bonds, our data showed that along the unfolding pathway the interaction with urea is maximal for protein conformations at intermediate values of R_{ca}.

The presence of intermediate conformations during the first stages of the unfolding process with an increased interaction with urea puts on quantitative grounds what has been earlier suggested as a "two-stage" mechanism by standard MD simulations.[20] Here, due to the use of an advanced sampling algorithm, we provide a quantitative proof of this picture for the case of the GB1 β-hairpin, which is a prototypical system for protein folding.

METHODS

System Setup. Following the work of Bussi et al.,[24] we used PTMetaD to study the folding/unfolding equilibrium of the β-hairpin protein in water and 8 M urea. We name the water solution as WS and the 8 M urea one as US. The protein coordinates were obtained from the C-terminus (residues 41−56) of protein G (PDB code 1G1B). The amino acid termini were capped: the N-terminal residue with an acetyl group (ACE) and the C-terminal residue with an *N*-methylamide capping group (NME). The protein was put in a rhombic dodecahedron box of ∼84 nm^3 volume in both the systems: in the WS 1834 water molecules were added, while in US we used 266 urea molecules and 1196 water molecules. Three Na^+ ions were also added to ensure charge neutrality in both systems. All simulations were performed using the GROMACS4MD code[41] and the PLUMED[42] plugin with the Amber99SB force field[27] for the protein, the flexible version of the OPLS-AA urea model for urea,[43,44] and the TIP3P model for water. A preliminary minimization and NPT simulation for 2 ns at 300 K and 1 atm was performed on both systems. A time step of 2 fs was used. All covalent bonds were constrained to their equilibrium value using the Lincs algorithm.[45] The electrostatic interactions were calculated by the particle mesh Ewald algorithm, and the Lennard-Jones interaction with a cutoff of 0.9 nm was used.

PTMetaD and the Reweighting Procedure. Metadynamics[46] is an advanced sampling algorithm based on the introduction of an external history-dependent bias potential in the space of a few CVs. In the PTMetaD technique multiple metadynamics simulations of the same system are performed in parallel. Each replica is simulated at a different temperature, and metadynamics bias is constructed on the same CVs. At fixed intervals, an exchange of configurations between two adjacent replicas is attempted on the basis of a Metropolis acceptance criterion. The exchange probability satisfies the detailed balance condition. By exchanging with higher temperatures, colder replicas are prevented from being trapped in local minima. In this way the free-energy profile is filled in parallel at all temperatures.

Here we used 64 replicas of both systems exponentially distributed in the temperature range of 270−695 K. All replicas were simulated in the NVT ensemble using a stochastic thermostat[47] with a coupling time of 0.2 ps. Exchanges were attempted every 0.2 ps. The resulting average acceptance probability was about 0.3 for all the replicas. Given the good results of Bussi et al.,[24] we used the same CVs of their work. The first CV is the radius of gyration calculated on the hydrophobic core (R_{core}). This is composed by four amino acids: Trp 43, Tyr 45, Phe 52, and Val 54. This collective variable is calculated using the following formula:

$$R_{core} = \left(\frac{\sum_i^n |r_i - r_{com}|^2}{\sum_i^n m_i} \right)^{1/2} \quad (1)$$

where the sums are over the n atoms and the center of mass is defined by

$$r_{com} = \frac{\sum_i^n r_i m_i}{\sum_i^n m_i} \quad (2)$$

The gyration radius is a common descriptor in protein folding studies because it is able to discriminate between a completely unfolded protein and a molten globule state, where the protein is compact but disordered. To distinguish between molten globule and folded states, we used as a second CV the number of intramolecular backbone−backbone H-bonds. The number of backbone H-bonds is evaluated using the switching function

$$H_{back} = \sum_{ij} \frac{1 - \left(\frac{d_{ij}}{r_0}\right)^n}{1 - \left(\frac{d_{ij}}{r_0}\right)^m} \quad (3)$$

where r_0 is set to 2.5 Å, n and m are set to 6 and 12, respectively, i and j are the hydrogen and oxygen backbone atoms used to calculate the number of H-bonds. We included in the CV only the H-bonds with a separation larger than 4 in the amino acidic sequence to study the parallel β-sheet formations.

Well-tempered metadynamics parameters were set as follows: the bias factor was set at 10 for each replica, and a Gaussian function was added every 1 ps with 0.05 and 0.025 widths for H_{back} and R_{core}. The initial Gaussian height was set to 1.0*T/270 kJ/mol. Each replica was simulated for 70 ns in the case of WS and 100 ns in the case of US.

To study the mechanism of urea denaturation, we have used the reweighting algorithm[26] that allows the unbiased probability distribution of any variable to be recovered from a well-tempered metadynamics simulation. In fact, the introduction of a bias potential, if properly done, leads to the correct distribution for the chosen CVs, but distorts that of the other degrees of freedom. The method is able to reconstruct the Boltzmann distribution of a fast variable directly from the configurations produced in a well-tempered metadynamics run where a time-dependent bias potential is added on the slow degrees of freedom of the system. From this relation all quantities of interest can be evaluated. In particular, quantitative comparison with experimental data is thus possible. In a previous work[48] the potential of this approach was shown by characterizing the conformational ensemble explored by a 13-residue helix-forming peptide by means of a well-tempered metadynamics/parallel tempering approach and comparing the reconstructed nuclear magnetic resonance scalar couplings with experimental data. The advantage of this reweighting procedure is not only to quantitative compare simulation with experimental data but also to save computer time because with this procedure any degrees of freedom different from CVs can be analyzed without performing additional metadynamics runs. In our case the use of the reweighting algorithm has allowed us to estimate, by a postprocessing procedure, the FES for important variables related to the mechanism by which urea performs its action. For both WS and US we have studied the FES as a function of the following variables (see the Supporting Information for the details): (1) radius of gyration calculated on all the Cα atoms (R_{ca}) and the distance from the crystallographic state in contact map space (Z_{map}); (2) total number of H-bonds between the backbone polar groups and solvent ($HB_{bb-solv}$) and R_{ca}; (3) number of all intramolecular H-bonds within the backbone polar groups (HB_{tot}) and R_{ca}; (4) number of non-native H-bonds (HB_{nonnat}) calculated as the difference between HB_{tot} and the number of native H-bonds and R_{ca}; (5) solvent-accessible surface (SAS), calculated by means of the g_sas tool of Gromacs[41] on the hydrophobic side chains of Trp, Tyr, Val, and Phe; (6) to understand the urea mechanism of action we also reweighted in two separated FESs the

contribution of H-bonds between the backbone polar groups and water (HB_{bb-wat}) and those between the backbone polar groups and urea (HB_{bb-ure}) as a function of R_{ca}.

■ ASSOCIATED CONTENT

Supporting Information. Deeper description of well-tempered metadynamics, details about the collective variables used in the reweighting procedure, convergence of the PTMetaD simulations, role of the side chain interactions with the solvent, and analysis of the protein−solvent potential energy. This material is available free of charge via the Internet at http://pubs.acs.org.

■ AUTHOR INFORMATION

Corresponding Author
alessandro.barducci@phys.chem.ethz.ch

■ ACKNOWLEDGMENT

Computational time for this work was provided by the Swiss National Supercomputing Center (CSCS). We thank Prof. Ben Schuler for useful discussions and critical reading of the manuscript. We also thank Mario Valle for his help with the graphics. Finally, we acknowledge the support of Grant ERC-2009-Ad4-247075.

■ REFERENCES

(1) Bolen, D.; Rose, G. *Annu. Rev. Biochem.* **2008**, *77*, 339–362.
(2) England, J.; Haran, G. *Annu. Rev. Phys. Chem.* **2011**, *62*, 257–77.
(3) Rupley, J. *J. Phys. Chem.* **1964**, *68*, 2002–2003.
(4) Frank, H.; Franks, F. *J. Chem. Phys.* **1968**, *48*, 4746–4757.
(5) Vanzi, F.; Madan, B.; Sharp, K. *J. Am. Chem. Soc.* **1998**, *120*, 10748–10753.
(6) Zhang, W.; Capp, M.; Bond, J.; Anderson, C.; Record, M. *Biochemistry* **1996**, *35*, 10506–10516.
(7) Courtenay, E.; Capp, M.; Record, M. *Protein Sci.* **2001**, *10*, 2485–2497.
(8) Bennion, B.; Daggett, V. *Proc. Natl. Acad. Sci. U.S.A.* **2003**, *100*, 5142–5147.
(9) Caballero-Herrera, A.; Nordstrand, K.; Berndt, K.; Nilsson, L. *Biophys. J.* **2005**, *89*, 842–857.
(10) Makhatadze, G.; Privalov, P. *J. Mol. Biol.* **1992**, *226*, 491–505.
(11) Mountain, R.; Thirumalai, D. *J. Am. Chem. Soc.* **2003**, *125*, 1950–1957.
(12) O'Brien, E.; Dima, R.; Brooks, B.; Thirumalai, D. *J. Am. Chem. Soc.* **2007**, *129*, 7346–7353.
(13) Lim, W.; Rösgen, J.; Englander, S. *Proc. Natl. Acad. Sci. U.S.A.* **2009**, *106*, 2595–2600.
(14) Wallqvist, A.; Covell, D.; Thirumalai, D. *J. Am. Chem. Soc.* **1998**, *120*, 427–428.
(15) England, J.; Lucent, D.; Pande, V. *J. Am. Chem. Soc.* **2008**, *130*, 11838–11839.
(16) Zangi, R.; Zhou, R.; Berne, B. *J. Am. Chem. Soc.* **2009**, *131*, 1535–1541.
(17) Stumpe, M.; Grubmüller, H. *J. Am. Chem. Soc.* **2007**, *129*, 16126–16131.
(18) Stumpe, M.; Grubmüller, H. *PLoS Comput. Biol.* **2008**, *4*, e1000221.
(19) Stumpe, M.; Grubmüller, H. *Biophys. J.* **2009**, *96*, 3744–3752.
(20) Hua, L.; Zhou, R.; Thirumalai, D.; Berne, B. *Proc. Natl. Acad. Sci. U.S.A.* **2008**, *105*, 16928–33.
(21) Canchi, D.; Paschek, D.; Garcia, A. *J. Am. Chem. Soc.* **2010**, *132*, 2338–2344.
(22) Canchi, D.; Garcia, A. *Biophys. J.* **2011**, *100*, 1526–1533.
(23) Laio, A.; Parrinello, M. *Proc. Natl. Acad. Sci. U.S.A.* **2002**, *99*, 12562.
(24) Bussi, G.; Gervasio, F.; Laio, A.; Parrinello, M. *J. Am. Chem. Soc.* **2006**, *128*, 13435–13441.
(25) Barducci, A.; Bussi, G.; Parrinello, M. *Phys. Rev. Lett.* **2008**, *100*, 20603.
(26) Bonomi, M.; Barducci, A.; Parrinello, M. *J. Comput. Chem.* **2009**, *30*, 1615–1621.
(27) Hornak, V.; Abel, R.; Okur, A.; Strockbine, B.; Roitberg, A.; Simmerling, C. *Proteins: Struct., Funct., Bioinf.* **2006**, *65*, 712–725.
(28) Jorgensen, W.; Tirado-Rives, J. *J. Am. Chem. Soc.* **1988**, *110*, 1657–1666.
(29) Munoz, V.; Thompson, P.; Hofrichter, J.; Eaton, W. *Nature* **1997**, *390*, 196–199.
(30) Blanco, F.; Rivas, G.; Serrano, L. *Nat. Struct. Mol. Biol.* **1994**, *1*, 584–590.
(31) Blanco, F.; Serrano, L. *Eur. J. Biochem.* **1995**, *230*, 634–649.
(32) Sinha, K.; Udgaonkar, J. *J. Mol. Biol.* **2005**, *353*, 704–718.
(33) Mayor, U.; Günter Grossmann, J.; Foster, N.; Freund, S.; Fersht, A. *J. Mol. Biol.* **2003**, *333*, 977–991.
(34) Li, Y.; Picart, F.; Raleigh, D. *J. Mol. Biol.* **2005**, *349*, 839–846.
(35) Nettels, D.; Müller-Späth, S.; Küster, F.; Hofmann, H.; Haenni, D.; Rüegger, S.; Reymond, L.; Hoffmann, A.; Kubelka, J.; Heinz, B.; Gast, K.; Best, R.; Schuler, B. *Proc. Natl. Acad. Sci. U.S.A.* **2009**, *106*, 20740–5.
(36) Merchant, K.; Best, R.; Louis, J.; Gopich, I.; Eaton, W. *Proc. Natl. Acad. Sci. U.S.A.* **2007**, *104*, 1528–33.
(37) Schuler, B.; Eaton, W. *Curr. Opin. Struct. Biol.* **2008**, *18*, 16–26.
(38) Bonomi, M.; Branduardi, D.; Gervasio, F.; Parrinello, M. *J. Am. Chem. Soc.* **2008**, *130*, 13938–13944.
(39) Holthauzen, L. M. F.; Roesgen, J.; Bolen, D. W. *Biochemistry* **2010**, *49*, 1310–1318.
(40) Auton, M.; Holthauzen, L. M. F.; Bolen, D. W. *Proc. Natl. Acad. Sci. U.S.A.* **2007**, *104*, 15317–15322.
(41) Hess, B.; Kutzner, C.; van der Spoel, D.; Lindahl, E. *J. Chem. Theory Comput.* **2008**, *4*, 435–447.
(42) Bonomi, M.; Branduardi, D.; Bussi, G.; Camilloni, C.; Provasi, D.; Raiteri, P.; Donadio, D.; Marinelli, F.; Pietrucci, F.; Broglia, R.; M., P. *Comput. Phys. Commun.* **2009**, *180*, 1961–1972.
(43) Duffy, E.; Severance, D.; Jorgensen, W. L. *Isr. J. Chem.* **1993**, *3*, 323–330.
(44) Smith, L.; Berendsen, H.; van Gunsteren, W. *J. Phys. Chem. B* **2004**, *108*, 1065–1071.
(45) Hess, B.; Bekker, H.; Berendsen, H.; Fraaije, J. *J. Comput. Chem.* **1997**, *18*, 1463–1472.
(46) Barducci, A.; Bonomi, M.; Parrinello, M. *Wiley Interdiscip. Rev. Comput. Mol. Sci.* **2011**, *1*, 826–843.
(47) Bussi, G.; Donadio, D.; Parrinello, M. *J. Chem. Phys.* **2007**, *126*, 014101.
(48) Barducci, A.; Bonomi, M.; Parrinello, M. *Biophys. J.* **2010**, *98*, L44–L46.